Chemical Engineering Journal Advances 25 (2026) 100983

Contents lists available at ScienceDirect

Chemical Engineering Journal Advances

journal homepage: www.sciencedirect.com/journal/chemical-engineering-journal-advances

Mitigating ammonia emissions for a sustainable livestock farming by advances in membrane technology and modelling tools

Paula Calvo-de Diego *, María Cruz García-González, Mercedes Sánchez-Báscones, Beatriz Molinuevo-Salces *

Department of Agroforestry Sciences, ETSIAA, University of Valladolid, Avenida Madrid 44, 34004, Palencia, Spain

ARTICLE INFO

Keywords:
Gas permeable membranes
Ammonia emissions
Ammonia recovery
Python modelling
Air cleaning

ABSTRACT

With the agricultural sector contributing to 93 % of total ammonia emissions, the development of mitigation technologies is imperative for livestock farming. This study compared the nitrogen recovery performance of two novel gas-permeable membrane configurations: System 1 (S1), with external gas flow, and System 2 (S2), with internal gas flow. The influence of initial N concentration and exposure time on N recovery rates was investigated. The results established the markedly superior performance of S2, which achieved a N recovery rate of 237 g m^{-2} d^{-1}, outperforming the 154 g m^{-2} d^{-1} rate of S1. This peak rate represents a 7-fold increase when compared to previous results. Mathematical models derived from regression analysis were developed for S1 and S2 and indicating that the theoretical maximum performance of S2 was 1.8-fold higher than that of S1 (Maximum N recovery rates of 155.65 and 281.2 g N m^{-2} d^{-1} for S1 and S2, respectively). The enhanced efficiency of S2 is ascribed to its internal flow configuration, which promotes a superior nitrogen mass transfer rate across the membrane. This design demonstrated greater robustness in managing high nitrogen loads, positioning it as a highly promising technology for practical implementation in livestock operations.

1. Introduction

Ammonia emissions (AE) represent a persistent environmental challenge in Europe, showing only marginal reductions between 2005–2022, in stark contrast to other regulated pollutants [1,2]. Achieving the ambitious 2030 emission reduction targets, set forth in the National Emission Reduction Commitments Directive, necessitates increased efforts, particularly from the nine Member States currently failing to meet their 2020–2029 commitments [1,3,4]. Given that the agricultural sector is responsible for approximately 93 % of total AE, there is an urgent need for effective mitigation strategies, including better integration with other national policies, such as the strategic plans under the Common Agricultural Policy (CAP), to ensure a coherent approach [2,5]. These emissions contribute significantly to environmental degradation, including air pollution, soil acidification, and eutrophication.

In this context, technologies enabling nitrogen (N) recovery from AE are growing interest. These not only mitigate NH_3 emissions but also offer economic benefits by converting recovered N into valuable fertilizers. Among various Best Available Techniques (BAT) for N recovery, gas-permeable membrane (GPM) systems have emerged as a promising solution [6]. Technologies such as air stripping towers combined with acidic absorption [7], bio trickling filters and biofilters [8], adsorption with zeolites [9] and gas-permeable membrane (GPM) systems are among the prominent methods for N recovery. GPM technology has gained attention due to its ability to operate at atmospheric pressure without requiring pretreatments or chemical additives, unlike air stripping towers or struvite precipitation processes that rely on chemicals or high-pressure systems [10,11]. Its low energy consumption further positions GPM as a sustainable and cost-effective alternative for reducing AE from sources like livestock buildings (e.g., swine barns) and manure storage facilities [11,12]. The core principle involves a selective hydrophobic membrane facilitating ammonia diffusion from an N-rich gas stream to an acidic absorption solution, driven by a concentration

Abbreviations: AE, Ammonia emissions; ANOVA, Analysis of variance; BAT, Best Available Techniques; CAP, Common Agricultural Policy; EC, Electrical conductivity; e-PTFE, Expanded polytetrafluoroethylene; GPM, Gas-permeable membrane; N, Nitrogen; SM, Synthetic Manure; TAN, Total Ammonia Nitrogen; MSE, Mean Square Error.

* Corresponding authors.
E-mail addresses: paula.calvo.diego@estudiantes.uva.es (P. Calvo-de Diego), beatriz.molinuevo@uva.es (B. Molinuevo-Salces).

https://doi.org/10.1016/j.ceja.2025.100983

Available online 3 December 2025

gradient [10,15,16]. This combination of environmental and economic advantages makes GPM technology a leading solution for sustainable livestock farming.

The escalating costs and supply chain vulnerabilities of synthetic nitrogen fertilizers underscore the importance of N recovery technologies [13,14]. GPM systems, by efficiently capturing N from ammonia-rich atmospheres, produce ammonium salt fertilizers (commonly ammonium sulfate) that can offset operational costs and reduce reliance on conventional synthetic inputs.

Previous studies have proved the efficiency of GPM technology for N recovery from the atmosphere. In this sense, Soto-Herranz [10] investigated suspended GPM to recover N from the atmosphere, using synthetic manure as ammonia emitting solution at different concentrations. At the lowest initial TAN concentration of 3 g L^{-1}, for example, N recovery rates in the range of 6–7 g N m membrane$^{-2}{}_D{}^{-1}$ were reported [10]. When the concentration was increased to 6 g N L^{-1}, the recovery rate improved, yielding a range of 13–21.4 g N m membrane$^{-2}{}_D{}^{-1}$ [10]. Furthermore, a subsequent study demonstrated that GPM performance at this same 6 g N L^{-1}concentration could be enhanced to 24–25 g N $m^{-2}{}_D{}^{-1}$ through the optimization of operational parameters, such as increasing the acid flow rate [17]. Finally, at a concentration of 12 g N L^{-1}, the N recovery rate was found to be between 19 and 34 g N $m^{-2}{}_D{}^{-1}$ [17]. Collectively, these studies establish a comprehensive performance benchmark for this technology with synthetic manure, demonstrating a recovery potential that scales with concentration but is also highly sensitive to system optimization. Subsequently, Calvo-de Diego [18], developed a new GPM configuration based on a cartridge system that significantly improved those capture rates, achieving N recoveries in the range of 23–73 g N $m^{-2}{}_D{}^{-1}$ when using pig slurry as the emitting solution. These N capture rates were increased to 237 g N $m^{-2}{}_D{}^{-1}$ when using a synthetic ammonia solution as the emitting solution. These results highlighted the potential for enhanced performance offered by the cartridge system design. However, more research is needed to improve the GPM configuration to maximize N recovery from the atmosphere.

Previous research carried out by Calvo-de Diego [18], demonstrated a non-linear relationship between contact time (between the GPM and the ammonia rich atmosphere) and nitrogen recovery rate. Their results showed an initial increase, with the rate rising from 23 g N $m^{-2}{}_D{}^{-1}$ (60 min) to a peak of 73 g N $m^{-2}{}_D{}^{-1}$ (120 min), followed by a decline to 60 g N $m^{-2}{}_D{}^{-1}$ (240 min), using pig manure as the emitting solution Calvo-de Diego et al. [18]. The dynamics of nitrogen emission from the pig manure, which are governed by its buffering capacity could explain this behavior. However, it is important to conduct further studies that generate different nitrogenous atmospheres, specifically by working with N-emitting solutions at varying concentrations, to better understand the dynamics of ammonia capture by GPM technology.

The objective of this study was to investigate different configurations of a novel cartridges system based on GPM technology for N recovery in N-rich atmospheres within the framework of the LIFE Green Ammonia Project. The study aims to compare two different configurations of this innovative GPM system: (1) an acidic trapping solution circulating inside the membrane with a NH_3-rich air flowing outside the membrane, and (2) an acidic trapping solution circulating outside the membrane with a NH_3-rich air flowing inside the membrane. The effects of N concentration in the atmosphere and the experimental exposure time of the membrane over the N recovery rate were evaluated for both configurations. Moreover, the effect of manure aeration time on ammonia emissions release was investigated for both systems.

2. Materials and methods

2.1. Synthetic manure (SM) characterization

To simulate swine manure for experimental purposes, a synthetic wastewater solution was meticulously formulated, named synthetic manure (SM). This solution was designed to closely mimic the characteristics of actual livestock effluent, with a specific focus on replicating two key parameters: Total Ammonia Nitrogen (TAN) and carbonate concentrations. A TAN of approximately 17.5 g N L^{-1} and a carbonate alkalinity level of approximately 18 g $CaCO_3L^{-1}$ were selected in accordance with Riaño [19]. The preparation process involved carefully measuring and dissolving precise quantities of two primary chemical compounds: 66.8 g of ammonium chloride (NH_4Cl) and 122 g of sodium bicarbonate ($NaHCO_3$) per liter of solution.

Different dilutions were made from the initial SM to obtain SM with lower concentrations (C1-C4). The characterization of the different SM used in the study is shown in Table 1.

Table 1
Chemical characterization of the different SM used for system 1 (S1) and system 2 (S2). Standard deviations between replicate analyses are indicated in parentheses.

		TAN g L^{-1}	pH -	EC mS cm^{-1}	Alkalinity g $CaCO_3$ L^{-1}
SM-S1	C1	2.93 (0.50)	9.0 (0.2)	33.8 (3.8)	14,693 (24.7)
	C2	5.74 (0.38)	9.1 (0.4)	63.2 (3.5)	25,835 (403.1)
	C3	8.96 (0.31)	9.1 (0.7)	90.4 (5.3)	43,133 (70.7)
	C4	17.29 (0.25)	8.6 (0.0)	145.0 (0.0)	68,363 (2139)
SM-S2	C1	2.80 (0.23)	9.1 (0.2)	34.1 (4.7)	14,693 (24.7)
	C2	5.53 (0.41)	9.0 (0.2)	59.2 (5.2)	25,835 (403.1)
	C3	8.77 (0.72)	9.4 (0.6)	88.0 (3.3)	43,133 (70.7)
	C4	17.31 (0.06)	8.8 (0.0)	142.8 (0.0)	68,363 (2139)

2.2. Experimental design

2.2.1. System 1. GPM system with the NH_3-rich air outside the membranes and the acidic trapping solution inside the membranes

System 1 (S1) was designed to capture NH_3 from the air and it is shown in Fig. 1. This system was compound by two cartridges (Cartridge 1 and Cartridge 2) with a GPM inside each cartridge (GPM 1 and GPM 2). The membranes used were made of expanded polytetrafluoroethylene (e-PTFE), a material known for its high hydrophobicity and thermal stability. The membranes had an outside diameter of 5 mm and a wall thickness of 0.5 mm. Key physicochemical properties included a high maximum continuous working temperature (260 °C), negligible water absorption (<0.01 %), and a low coefficient of friction, which are advantageous for long-term operation in demanding environments. The membrane had a length of 1 m The membrane's surface area was 0.0157 m^2, which was calculated considering the outside diameter. In S1, the NH_3-rich air was conducted throughout the space between the outside of the membrane and the inner part of the cartridges. To generate an NH_3-rich atmosphere, a volume of 500 ml of SM was aerated in the ammonia generation tanks (Ammonia generation tank 1 and ammonia generation tank 2). The aeration was carried out with a vacuum pump (DOA-P504-BN, Gast Manufacturing, INC, Mich. U.S.A), which recirculated the air from the end of the cartridges to aerate the SM with a continuous air flow connected to porous stones giving an aeration flow rate of 8 L min^{-1}. Then, the NH_3 was allowed to enter the capture system, where the GPM was located. The acidic trapping solution (a solution of sulphuric acid 1 N) was introduced inside the membrane by a peristaltic pump (Heidolph, Peristaltic Pump, Hei-FLOW Value 01 EU, Germany) and it remained static inside the membrane all the experimental time. Once the experiment was completed, the acidic trapping solution was extracted from the other end of the cartridge, propelled by the same peristaltic pump that introduced it into the membrane, allowing the determination of the captured N.

A total of 13 duplicated tests were run to study the effect of ammonia concentration in the air and experimental time on the performance of S1. More specifically, tests were conducted with SM at four N concentrations, namely C1, C2, C3 and C4 (Table 1) at different experimental times. For C1 test durations of 60, 120, 180 and 300 min were performed. For C2 test durations of 60, 120, and 180 min were carried out.

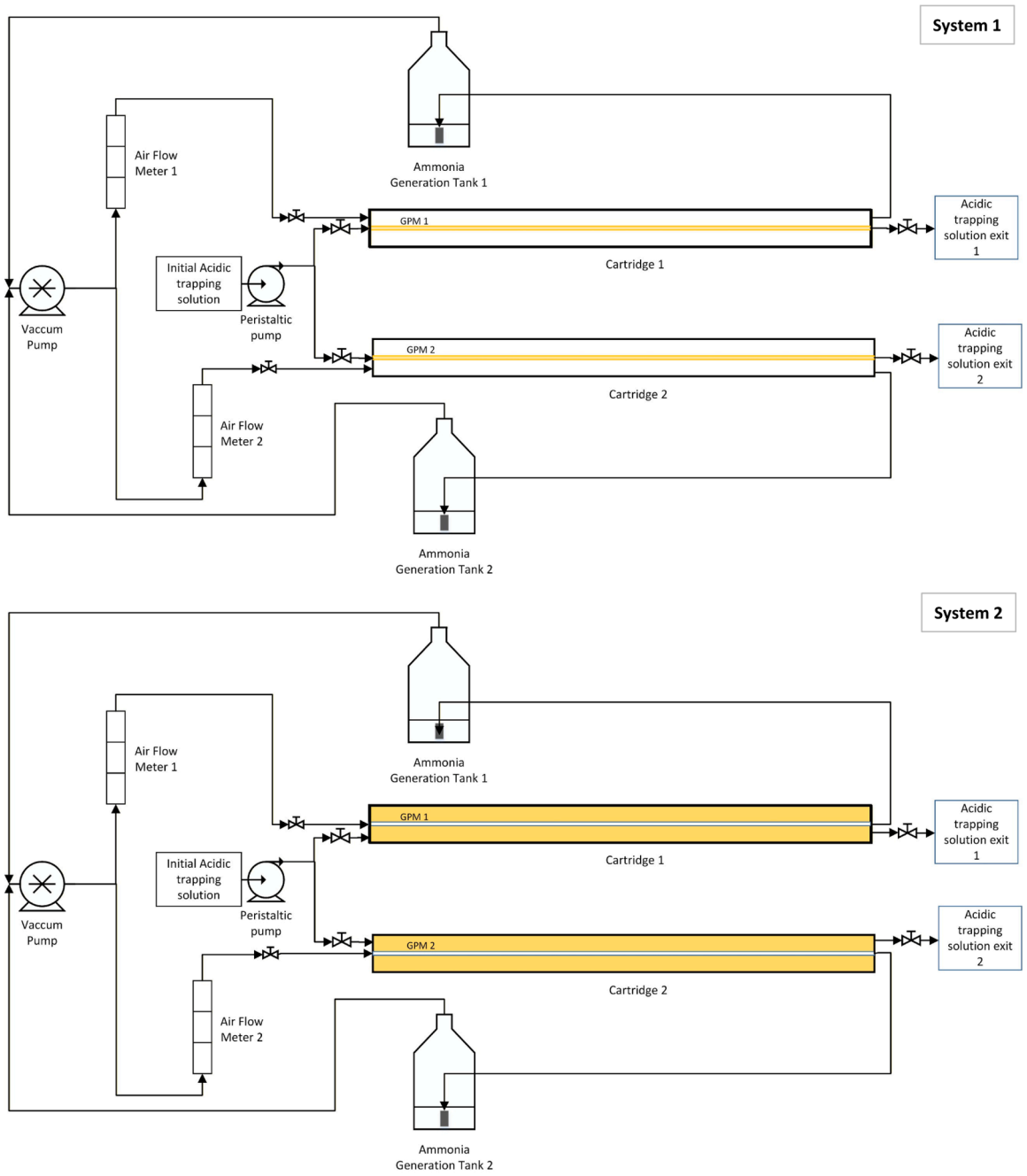

Fig. 1. GPM systems of cartridges.

For C3, test durations of 60, 120, 180, 240 and 300 min were run. For C4, a test with a duration of 120 min was run. Upon completion of each test, the ammonia generation tanks were opened and a sample from the final SM was collected for the determination of TAN concentration, allowing for a mass balance of the emitted TAN. Each sample was analyzed in duplicate. From the acidic trapping solution, a sample was extracted analysis of its TAN content, allowing the determination of the captured TAN. Each sample was analyzed in duplicate. The initial and final pH and electrical conductivity (EC) of the SM were measured. The pH of the acidic trapping solution was also recorded at the beginning and end of each test.

2.2.2. System 2. GPM system of cartridges with the NH_3-rich air inside the membranes and the acidic trapping solution outside the membranes

System 2 (S2) was identical to system 1 (Fig. 1). The fluid configuration on both sides of the membrane was reversed than S1. Specifically, the NH_3-rich air flowed through the inside of the membrane at the same rate as in system 1, 8 L min^{-1}, while the acidic trapping solution remained static inside the cartridges on the exterior side of the GPM.

A total of 11 duplicated tests were run to study the effect of ammonia concentration in the air and experimental time on the performance of S2. More specifically, tests were conducted with SM at four TAN concentrations, namely C1, C2, C3and C4 (Table 1) at different experimental times. For C1 test durations of 60, 120 and 180 min were performed. For C2 test durations of 60, 120, and 180 min were carried out. For C3, test durations of 60, 120, 180 and 300 min were run. For C4, a test with a duration of 120 min was run.

To ensure a comprehensive understanding of the dynamic behavior of the systems, the duration of the experiments was initially established

Table 2
Experimental data for system 1 (S1). Standard deviations between replicate tests are indicated in parentheses.

Synthetic Manure				Acidic Trapping Solution			
Initial TAN	Time	Final EC	Final pH	Emitted N	Air N concentration	Final pH	N recovery
g L^{-1}	min	mS cm^{-1}	-	mg	mg L^{-1} min^{-1}	-	%
C1	60	29.8(2.9)	9.6(0.5)	220.5(29.1)	1.4(0.2)	0.22(0.01)	36.2(4.7)
	120	30.4(3.0)	9.3(0.0)	355.5(79.2)	1.1(0.2)	0.62(0.04)	39.0(1.7)
	180	37.8(0.1)	9.0(0.0)	385.5(4.2)	0.8(0.0)	0.77(0.09)	79.1(0.2)
	300	28.7(0.0)	9.3(0.0)	419.0(75.0)	0.5(0.1)	1.1(0.06)	85.7(1.5)
C2	60	58.2(1.2)	9.7(0.0)	292.5(34.7)	1.8(0.2)	0.5(0.04)	30.9(8.0)
	120	59.5(1.1)	9.6(0.0)	410.5(167.6)	1.3(0.5)	0.6(0.01)	37.4(4.5)
	180	66.7(0.1)	8.8(0.0)	471.5(228.4)	1.0(0.5)	1.1(0.14)	54.9(0.5)
C3	60	83.9(1.9)	10.1(0.0)	762.8(41.4)	4.7(0.3)	0.8(0.04)	10.5(2.0)
	120	71.0(0.4)	10.2(0.1)	707.8(47.5)	2.2(0.1)	1.4(0.22)	38.5(3.4)
	180	98.0(0.4)	8.6(0.0)	409.0(84.1)	0.8(0.2)	1.6(0.02)	92.1(2.6)
	240	80.7(0.1)	9.2(0.0)	682.0(84.9)	1.1(0.1)	1.7(0.07)	58.2(2.4)
	300	80.9(0.5)	9.3(0.0)	716.0(31.8)	0.9(0.0)	2.6(0.11)	61.9(0.4)
C4	120	140.7(0.4)	9.1(0.02)	554.5(119.5)	1.7(0.4)	1.7(0.04)	72.9(1.0)

for both GPM configurations. Following the initial experiments, it was found that System 1 exhibited greater variability across different time points. Consequently, additional intermediate experimental durations were designed specifically for System 1, to thoroughly characterize its recovery dynamics under various conditions. System 2, demonstrating a more consistent performance profile, did not require the same number of intermediate trials. The same samples were taken and the same analyses as in System 1 were carried out.

2.3. Analytical methods and yields

TAN concentration was analyzed by Kjeldahl method, by steam distillation followed by collection of the distillates in borate buffer and titration with 0.2 M HCl. A Kjeltec 8100 apparatus (Foss Iberia S.A., Barcelona, Spain) was used for distillation. pH, Electrical Conductivity and total alkalinity were monitored using a GLP22 electrode (Crison Instruments S.A., Barcelona, Spain). Total alkalinity (TA) was determined by measuring the amount of standard sulfuric acid needed to bring the sample to pH of 4.5.

The amount of emitted N was determined as the difference in Total Ammoniacal Nitrogen (TAN) concentration in the SM. The calculation used the final measured sample volume to correct any volume losses that occurred during the experiment. Emitted N (mg) was calculated following Eq. (1):

$$Emitted\ N\ (mg) = TAN_{initial}\left(mg.L^{-1}\right) * V_{initial}(L) - TAN_{final}\left(mg.L^{-1}\right) * V_{final}(L) \quad (1)$$

Where $TAN_{initial}$ corresponds to the total ammonia nitrogen initial in mg L^{-1} and $V_{initial}$ is the initial volume of SM in L and TAN_{final} final corresponds to the total ammonia nitrogen final in mg L^{-1} and V_{final} is the final volume of SM in L.

Emitted N (%) was calculated following Eq. (2):

$$Emitted\ N\ (\%) = \frac{Emitted\ nitrogen\ (mg)}{TAN_{initial}\ (mg)} * 100 \quad (2)$$

N recovery (%) was calculated following Eq. (3):

$$N\ recovery\ (\%) = \frac{Recovered\ nitrogen\ (mg)}{TAN_{initial}\ (mg)} * 100 \quad (3)$$

Where recovered nitrogen (in mg) corresponds to the amount of N captured by the acidic trapping solution.

N recovery rate (g $m^{-2}{}_D{}^{-1}$) was calculated following Eq. (4):

$$N\ recovery\ rate\ \left(g\ m^{-2}\ d-1\right) = \frac{Recovered\ nitrogen\ (mg)}{Superficial\ Membrane\ Area(m^2) * Time(days) * 1000\left(\frac{mg}{g}\right)} \quad (4)$$

Air N concentration in the atmosphere systems was calculated following Eq. (5)

$$Air\ N\ concentration\ \left(mgL^{-1}min^{-1}\right) = \frac{Emitted\ nitrogen\ (mg)}{Time\ (min)\ *\ Air\ volume\ (L)} \quad (5)$$

Where $Airvolume(L)$ is the total volume for gas circulation within the systems. In the case of System 1 the value was 1.344 L (volume was calculated by adding: the external volume of the membrane in the cartridge, the volume occupied by the gas in the aeration tank, and the internal volume of the pipes), whereas for System 2 it was 0.586 L (volume was calculated by adding: the internal volume of the membrane in the cartridge, the volume occupied by the gas in the aeration tank, and the internal volume of the pipes).

2.4. 3D visualization and mathematical modeling of N recovery rate

To visualize the performance of S1 and S2 and to derive their respective behavioral equations, a custom Python script was developed and executed within the Google Collab environment. This script was designed to process data from TAN initial concentration (g TAN L^{-1}), time test (minutes) and N recovery rate (g N $m^{-2}{}_D{}^{-1}$). Upon execution,

Table 3
Experimental data for system 2 (S2). Standard deviations between replicate tests are indicated in parentheses.

Synthetic Manure				Acidic Trapping Solution			
Initial TAN	Time	Final EC	Final pH	Emitted N	Air N concentration	Final pH	N recovery
g L^{-1}	min	mS cm^{-1}	-	mg	mg $_L^{-1}$ min^{-1}	-	%
C1	60	29.5(1.2)	9.3(0.01)	136.7(59.6)	1.9(0.8)	0.05(0.01)	37.5(4.7)
	120	30.1(1.2)	9.2(0.02)	298.5(125.2)	2.1(0.9)	0.05(0.01)	104.7(28.0)
	180	36.4(0.4)	9.1(0.04)	494.0(94.8)	2.3(0.4)	0.05(0.0)	92.9(7.1)
C2	60	63.1(2.3)	9.3(0.07)	223.0(50.6)	3.2(0.7)	0.04(0.01)	73.4(9.1)
	120	63.5(2.6)	9.0(0.33)	380.0(101.1)	2.7(0.7)	0.02(0.0)	101.5(25.7)
	180	52.7(0.2)	9.5(0.01)	556.0(4.2)	2.6(0.0)	0.15(0.0)	103.4(22.9)
C3	60	83.3(0.1)	10.2(0.08)	334.2(52.0)	4.7(0.7)	0.15(0.02)	93.0(16.6)
	120	84.5(0.4)	10.1(0.04)	676.5(98.3)	4.8(0.7)	0.12(0.01)	84.5(10.0)
	180	83.0(0.7)	9.4(0.04)	889.0(121.6)	4.2(0.6)	0.14(0.01)	95.0(27.2)
	300	74.4(0.2)	9.2(0.06)	1622.0(137.9)	4.6(0.4)	0.10(0.0)	70.8(2.9)
C4	120	141.1(0.1)	9.2(0.06)	909.0(9.9)	6.5(0.1)	0.16(0.0)	56.8(5.5)

the script generated a three-dimensional scatter plot to represent the interdependencies of these variables. Furthermore, the script performed a regression analysis to establish a mathematical model, yielding an equation that describes the N recovery rate as a function of time test and TAN initial concentration.

2.5. Statistical analyses

An analysis of variance (ANOVA) was used to determine the statistical analysis of the experimental data (TAN initial SM, Test time, TAN recovery and N Recovery Rate). To determine statistical significance, the 95 % confidence interval of differences ($p < 0.05$) was chosen. Residual normality and homoscedasticity were evaluated via the Shapiro-Wilk test. To meet the assumptions of parametric tests, a subset of the studied variables underwent logarithmic transformation to approximate a normal distribution. All statistical operations were executed within the R Studio environment (version 3.4.3).

3. Results and discussion

3.1. Effect of aeration time on NH_3 emission for systems 1 and 2

Table 2 presents experimental data for the four TAN concentrations in synthetic manure (C1, C2, C3 and C4) with different test durations in each case.

The final electrical conductivity (EC) of the SM varied according to initial TAN concentrations and test durations. A consistent observation across all trials was a decrease in EC from the initial values (Table 1), correlating with the reduction in N concentration within the SM. This diminution in EC during aeration is principally attributed to the loss of dissolved ionic species. Crucially, the volatilization of ammonia gas (NH_3) leads to a reduction in the concentration of ammonium ions (NH_4^+) in the solution [17,20,21]. As NH_4^+ ions are significant contributors to electrical conductivity, their depletion directly results in lower EC values. At the end of the tests, a consistent increase in the pH of the SM was observed across experimental conditions. The pH in SM was measured across experimental conditions. It was observed that the final pH was higher at shorter experimental times than at longer ones, as exemplified by experiment C3 (Table 2), exception made for C3 at 180 min, which exhibited a final pH of 8.6. This observed pH evolution in the SM can be attributed to two distinct processes occurring during low-rate aeration. Initial increase in pH is primarily attributed to the rapid removal of dissolved carbon dioxide (CO_2) from the solution, as CO_2 is stripped away, the concentration of carbonic acid decreases, leading to a reduction in overall acidity and an increase in the pH [21,22]. The exception to this general trend observed for C3 at 180 min, which exhibited a final pH of 8.6, is believed to be due to an incomplete consumption of CO_2 at this time point, in contrast to other experimental conditions. This is further supported by the higher electrical conductivity (EC) observed, indicating a different ionic balance and it could be due to technical issues during the aeration. Consequently, the emission of N was also lower for this specific trial, which counterintuitively

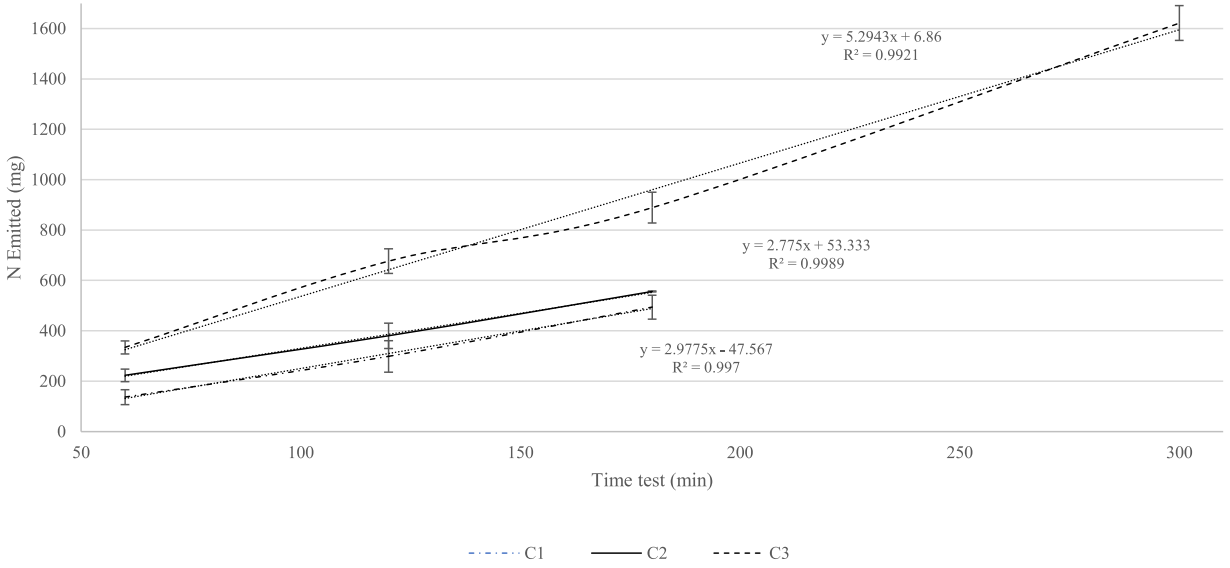

Fig. 2. N emitted in System 2 C1, C2 and C3 across varying test durations.

resulted in a higher percentage of recovery compared to other experiments at similar conditions.

However, as the aeration continues, the slower but ultimately dominant process of ammonia (NH_3) volatilization takes over. The removal of gaseous NH_3 from the liquid phase forces the chemical equilibrium ($NH_4^+ \rightleftharpoons NH_3 + H^+$) to shift to the right, resulting in the continuous and progressive release of hydrogen ions (H^+). The accumulation of these H^+ gradually acidifies the solution, which explains the subsequent decrease in pH over an extended operational period [23].

The quantity of emitted TAN varied depending on the initial TAN concentration (C1-C4), test duration and final pH of SM. Generally, TAN emissions increased with progressive aeration time across all initial TAN concentrations, with higher initial SM concentrations typically resulting in greater cumulative N release. For instance, in the C1 test, emitted N increased from 220.5 mg at 60 min to a peak of 419.0 mg after 300 min. With regards to air N concentration, it was found to be highest during shorter experimental time, a trend that directly correlates with the pH evolution. Specifically, the most pronounced pH increases were recorded in these initial stages, thus driving higher emissions. As the experiment progressed, pH levels stabilized or decreased, resulting in the subsequent attenuation of the N emitted, as discussed previously. The C2 test exhibited a similar trend, with emissions rising from 292.5 mg to a maximum of 471.5 mg at 180 min. The C3 test reported N emissions of 762.8 mg and 707.8 mg within the 60 and 120 min. At 180 and 300 min, C3 test showed values of 409.0 mg and 716.0 mg, respectively. This is attributed to the fact that the 60 min and 120 min tests reached higher pH than the others (Table 2), thereby favoring ammonia emission due to a shift in the equilibrium. Consequently, the N capture percentages varied with emission. For the C3 60 min test, despite high initial emissions due to elevated pH, the shorter operational time was insufficient for complete N capture. In the C3 120 min test, N emitted was nearly identical to the C3 60 min test, but the extended experimental duration facilitated a higher N capture percentage. Conversely, the C3 180 min test achieved the lowest final pH, resulting in reduced N emitted and consequently, the highest recovery efficiency. For the C3 240 min and 300 min tests, N emitted were comparable to the 60 min and 120 min tests, as the final pH was not as high. However, the increased experimental time allowed for an improved N capture percentage.

For C4, an N emission of 554.5 mg was recorded at 120 min. Despite a higher initial ammonium ion concentration, the C4 test began at a lower pH and did not reach comparably high pH values. Therefore, the N emitted from C4 was not greater than that from C3 at 120 min, for instance. These findings strongly suggest that higher pH levels facilitate enhanced nitrogen volatilization, particularly during the initial stages of aeration, by promoting the conversion of ammonium to volatile ammonia under alkaline conditions. Conversely, lower pH values likely mitigate nitrogen emissions by favoring the more stable, non-volatile ammonium ion (NH_4^+), thereby retarding the volatilization process.

Table 3 presents the experimental data for S2 for the four concentrations (C1, C2, C3 and C4) across varying test durations.

The final EC exhibited a direct relationship with SM concentration. A decrease in EC relative to the initial value (Table 1) was observed for all concentrations, which is attributed to the same mechanism described for S1. The final pH obtained different values depending on the SM concentrations and test times. A reduction in pH with experimental time was observed, as observed in S1, can likely be attributed to the previously described discussion involving two distinct processes occurring during aeration. Specifically, both setups involved gas recirculation, where the gas was bubbled back through the SM, the source of the emission. Contrary to S1, in S2 the emitted N increased proportionally with both SM concentration and time (Fig. 2). N emitted exhibited a direct linear correlation with both the SM concentration and the duration of the experiment (Fig. 2). For each synthetic manure concentration tested, the N emitted was plotted against the experimental time, revealing a consistent linear relationship across all concentrations. Air N concentration remained stable during the experimental time for each N concentration (exception made for C2 120 min), independently of the time test.

Table 4
N recovery rates for system 1 (S1) and system 2 (S2). Standard deviations between replicate tests are indicated in parentheses.

		N recovery rate	
Initial TAN SM	Time	S1	S2
g L^{-1}	min	g $m^{-2}d^{-2}$	
C1	60	61.0(7.8)	39.2(4.9)
	120	53.0(2.3)	119.4(31.9)
	180	77.7(0.2)	116.9(8.9)
	300	54.9(1.0)	-
C2	60	69.1(17.8)	125.0(15.5)
	120	58.6(7.1)	147.3(37.3)
	180	65.9(0.6)	146.5(32.4)
C3	60	61.2(11.7)	237.3(42.4)
	120	103.9(9.2)	218.3(25.7)
	180	95.9(2.7)	215.8(61.6)
	240	75.8(3.1)	-
	300	67.7(0.5)	175.6(7.2)
C4	120	154.3(2.1)	196.8(19.0)

A comparative analysis of the N air concentration for both systems revealed different operational dynamics between the two systems (Tables 2 and 3). S1 (ammonia outside the membrane) exhibited a declining N concentration in the air with experimental time. This trend was particularly pronounced in condition C3, where the flux sharply decreased from an initial peak of 4.7 mg L^{-1} min^{-1} to just 0.8 mg L^{-1} min^{-1} after 180 min (Table 2). In stark contrast, S2 (ammonia inside the membrane), demonstrated a capacity to maintain a relatively stable and sustained N concentration in the air. For instance, under the same C3 condition for S2, N concentration in the air fluctuated within a narrow range of 4.2 to 4.8 mg L^{-1} min^{-1} throughout the experiment (Table 3). This comparison indicates that while both systems could achieve high initial emission rates at elevated TAN concentrations, S2 was significantly more effective at maintaining that high rate over time, whereas the emission process in S1 appeared to be rate-limited or depleted as the experiment progressed. An operational analysis based on a real farm scenario, processing continuous N-rich air from animal housing reveals fundamental differences in the gas residence time of each configuration. The gas volume in S1, corresponding to the internal cartridge volume and exterior to GPM, is 0.77 L, which at a flow rate of 8 L min^{-1} yields a residence time of 5.775 s. Conversely, the gas volume of S2 is confined to the GPM internal volume is 0.013 L, resulting in a residence time of 0.016 s. This constitutes a 361-fold greater residence time in S1 than in S2. The implication of this disparity is that S2 facilitates a significantly higher N recovery rate (Table 4). It is therefore concluded that for large-scale applications, such as treating the high-volume, N-rich air from a pig farm, the configuration of S2 is substantially more efficient.

Statistical analysis revealed a highly significant difference in the percentage of N recovery between System 1 and System 2. The extremely low p-value of 1.8×10^{-11}, well below the significance threshold of 0.05, allowed us to reject the null hypothesis and confidently conclude that a statistically significant disparity in N recovery exists between these two systems. The Shapiro-Wilk test for normality exceeded a p-value of 0.05, indicating that the data did not significantly deviate from a normal distribution. The substantial difference in N recovery between System 1 and System 2 is unequivocally supported by the remarkably small p-value derived from their direct comparison.

3.2. Effect of aeration time on TAN recovery for systems 1 and 2

N recovery percentages for S1 and S2 are presented in Tables 2 and 3, respectively. The pH of the acidic trapping solution increased as the concentration of captured nitrogen raised. In S1, higher final pH values were observed in the acidic trapping solution. This is attributed to the fact that the acidic solution volume was lower than that in S2, which led

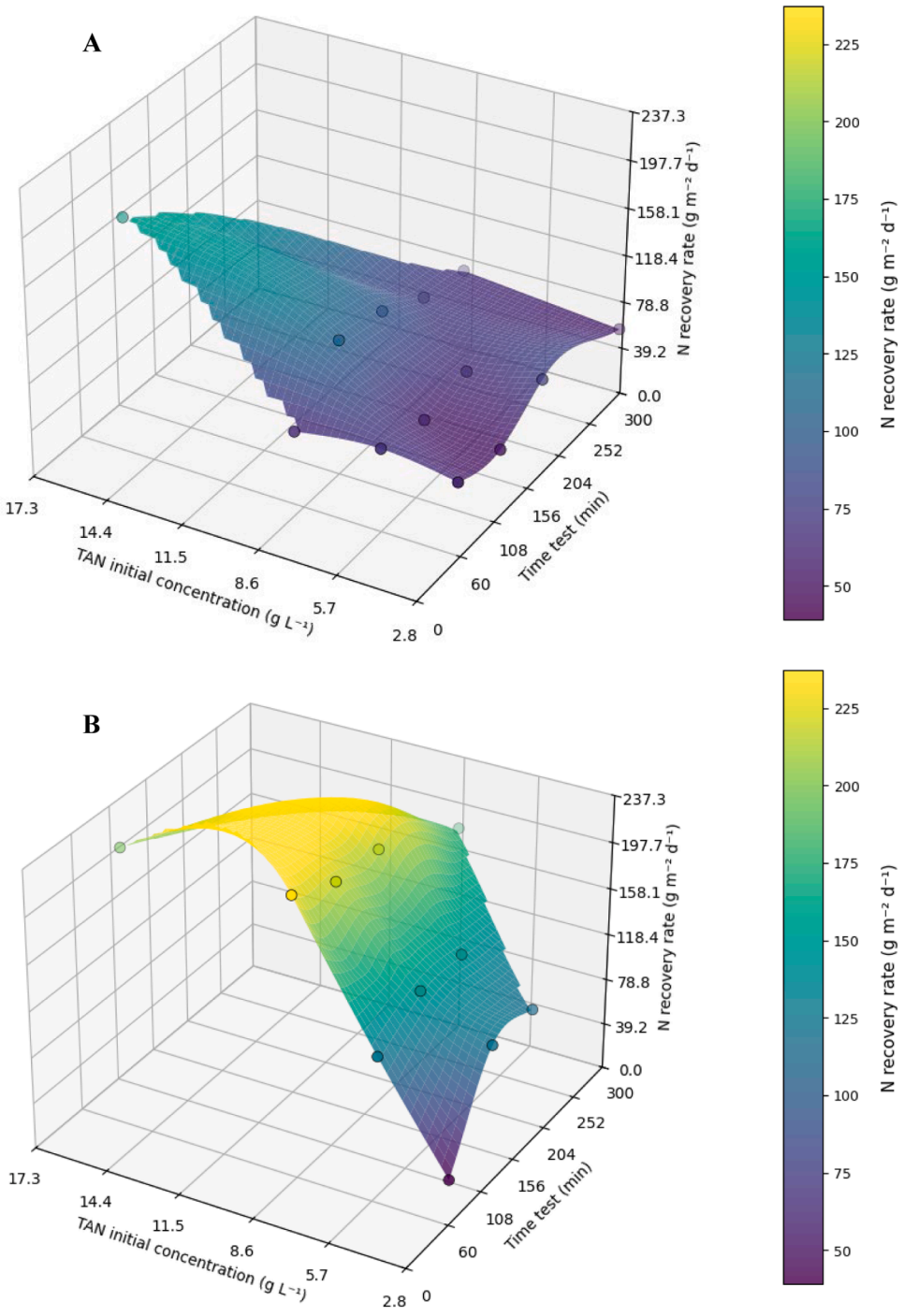

Fig. 3. 3D Visualization of N Recovery Rate for System 1 (2A) and System 2 (2B) for the four concentrations (C1, C2, C3 and C4) across varying test durations (60, 120, 180, 240, and 300 min).

to a more rapid increase in the captured nitrogen concentration. A direct correlation was established between the pH of the acidic trapping solution and the concentration of captured nitrogen. The progressive capture of ammonia (NH_3) leads to its conversion into ammonium ions (NH_4^+) within the acidic solution, a process that consumes H^+ ions. Consequently, as the concentration of captured nitrogen rises, the acidity of the solution is gradually neutralized, resulting in an observable increase in its pH [21]. In S1, N recovery percentage varied significantly depending on both initial TAN concentration and test duration (Table 2). More specifically, low TAN concentrations (C1) reached high N recovery percentages at long experimental times while high TAN concentrations (C3) reached high N recovery percentages at short experimental times. The observed trend in S1 can be explained by the dynamic interplay between the rate of N emission and the efficiency of the capture solution. Initially, a high emission flux may kinetically overwhelm the trapping system, resulting in a lower recovery percentage. As the experiment progresses, the capture process becomes more effective relative to the emission rate, causing the recovery percentage to increase. These results highlight how concentration influences recovery efficiency, with intermediate times yielding optimal results.

In S2 (Table 3), where the air N concentration remained consistently high in each initial TAN concentration, the N recovery percentage appears to be primarily governed by the duration of contact time. This is clearly illustrated by the results for condition C1: the initial recovery of

37.5 % at 60 min suggests that the contact time was insufficient for the system to effectively capture the available ammonia. By extending the duration to 120 min, the recovery percentage peaked at 104.7 %, indicating that the longer contact period allowed for more complete mass transfer across the membrane. This interpretation is further supported by the data from condition C2, where the high initial recovery of 73.4 % at 60 min, which subsequently increased to over 100 %, demonstrates that while the initial contact time was already highly effective, extending the operational period allowed the system to capture virtually all the N emitted. A plausible explanation is that a high nitrogen emission rate does not directly translate into an equally high capture rate. This may indicate that the capture process is kinetically limited, requiring sufficient contact time for the airborne nitrogen to be effectively trapped by the membrane. For instance, C3 system achieved 95.0 % recovery in 180 min, but prolonged treatment (300 min) reduced recovery to 70.8 %. At higher concentrations, emitted nitrogen levels were elevated, and efficiency decreased because the system cannot capture the entirety of the emitted nitrogen.

According to previous studies, Soto-Herranz [10] conducted tests to recover N from the atmosphere using SM at various initial TAN concentrations (3, 6 and 12 g L^{-1}) over 14 days, using a membrane area of 0.0164 m^2 (like that in the present study, 0.0157 m^2) and a membrane area of 0.0082 m^2. During the 14-day trial, emissions with an initial TAN concentration of 3 g L^{-1} ranged from 840 to 1655 mg N, with N recovery percentages of 79 % and 88 % for the two membrane areas, respectively. Notably, our study achieved an 86 % N recovery in just 180 min in S2, equivalent to approximately half and one-quarter of the 14-day emission values reported by Soto-Herranz [10] (840 mg and 1655 mg, respectively). This demonstrates that our novel system design (S1) can capture the same amount of N in a considerably shorter timeframe (<1 day) compared to Soto-Herranz [10], highlighting a significant improvement in N capture. When compared to the results obtained in this study for C1 (which utilized a similar initial TAN concentration), the N emission for S1 and S2 was notably higher in the present study. This can be attributed to the system's design, which inherently enhances the emission process. The enhancement likely occurs because the gas, now enriched with the emitted N, is continuously recirculated and bubbled back through the SM, promoting further volatilization through agitation.

With regards to 6 g L^{-1} SM concentration, Soto-Herranz [10] reported N emissions over a 14-day trial ranging from 1748 to 3106 mg N, yielding N recovery percentages of 88 and 96 %, respectively, for the two membrane areas studied (0.0164 m^2 and 0.0082 m^2). Furthermore, Soto-Herranz [17] reported an N emission of 3154 mg N and a N recovery of 88 % for a 7-day trial with a 6 g L^{-1} SM concentration using a surface area of 0.01634 m^2. When compared to the results obtained in the present study for C2, which utilized a similar initial TAN concentration, the N emission was notably higher in our study. This enhanced emission is attributed to the aeration applied in our system. Although, in S1, the N recovery percentage of 54.9 % achieved within 180 min in our study was lower than those reported by Soto-Herranz, it is anticipated that this recovery percentage will increase with longer trial durations. Consequently, the results observed in S1 and S2 represent a significant improvement over those documented in prior studies.

3.3. 3D visualization and mathematical modeling of N recovery rate for system 1 and system 2

The N recovery rates obtained in S1 and S2 are shown in Table 4 for the four concentrations (C1, C2, C3 and C4) across varying test durations.

Fig. 3 presents 3D Visualization of N recovery rate in relation to TAN concentration and test time for S1 (2A) and S2 (2B). In S1, the N recovery fluctuated between 53 and 104 g m^{-2} d^{-1} for C1, C2 and C3 concentrations. The highest recovery rate for S1 was 154.3 g m^{-2} d^{-1}, achieved at the highest concentration (C4). There was no consistent trend with respect to time within each experiment; but the rate often peaked at an intermediate time point before declining. For C1, N recovery rate ranged from 61 g $m^{-2}d^{-1}$ (at 60 min) to a peak of 77.7 g $m^{-2}d^{-1}$ (at 180 min), followed by a decline to 54.9 g $m^{-2}d^{-1}$ (at 300 min). For C2, N recovery rate was slightly higher overall, starting at 69.1 g $m^{-2}d^{-1}$ at 60 min and decreasing slightly at 58.6–65.9 g $m^{-2}d^{-1}$ around 120–180 min. For C3, N recovery rates were significantly greater, peaking early in the experiment (103 g $m^{-2}d^{-1}$) after just 120 min before decreasing between values of 95.9–67.7 g $m^{-2}d^{-1}$ for longer durations. In the case of the trials with SM of C4, it was observed that the N recovery rate obtained was 154.3 g $m^{-2}d^{-1}$, being higher than those obtained with SM of lower concentrations. Thus, in S1 for higher SM concentrations, a higher N recovery rate was obtained.

In contrast, S2 demonstrated a superior N recovery rate across all comparable conditions. Its rates were frequently double or even triple those of S1, typically ranging from 115 to a peak of 237 g N g $m^{-2}d^{-1}$. This finding confirms a far more effective and rapid capture of N per unit of area and time in S2. There is a statistically significant difference between the nitrogen recovery rates of the two systems. N recovery rates for S2 demonstrated a relation between SM concentration and time test. At C1, recovery rates increased from 39.2 g $m^{-2}d^{-1}$ (60 min) to 119.4 g $m^{-2}d^{-1}$ (120 min), stabilizing at 116.9 g $m^{-2}d^{-1}$ (180 min). The C2 tests exhibited higher rates, peaking at 147.3 g $m^{-2}d^{-1}$ (120 min) and maintaining 146.5 $m^{-2}d^{-1}$ (180 min). Elevated initial concentrations of C3, achieved the highest rates (ranging between 237.3–215.8 g $m^{-2}d^{-1}$ from 60 to 180 min), though rates slightly decreased to 175.6 g $m^{-2}d^{-1}$ (300 min). The C4 test achieved a removal rate of 196.8 g $m^{-2}d^{-1}$ (120 min), suggesting that higher SM concentrations do not necessarily yield greater N recovery rates, therefore, the N recovery rate is more directly influenced by the resulting air N concentration, rather than by the initial test conditions alone. This means that the efficiency of S2 configuration was far superior to that of S1. S2 performance was quantitatively and significantly more effective than that of S1 in recovering nitrogen per unit of membrane surface area and time.

Statistical analysis revealed a highly significant disparity in the N recovery rate between System 1 and System 2. The derived p-value of 3.75×10^{-13}, which is substantially lower than the significance level of 0.05, provided compelling evidence to reject the null hypothesis, thereby confirming a statistically significant difference in the N recovery rates between the two systems. Although the Shapiro-Wilk test for normality yielded a p-value exceeding 0.05, which indicates that the data did not significantly deviate from a normal distribution, the exceedingly small p-value from the direct comparison unequivocally establishes significant differences in N recovery rates between System 1 and System 2.

According to Fig. 3 the results presented herein clearly demonstrate a significant disparity in N recovery rate between S1 and S2 when evaluated under identical ranges of time test (60–300 min) and TAN initial concentration (3–18 g L^{-1}.). In both systems, the N recovery rate generally increased with longer operational times and higher initial TAN concentrations, as visualized by the 3D surface response plots, although they were far superior in the case of the S2. These findings align with fundamental mass transfer principles, wherein an augmented TAN concentration gradient and prolonged contact duration are expected to enhance N transfer. The primary differentiating factor between the systems, however, was the magnitude of the N recovery rate. S1, as depicted in its respective 3D surface plot, yielded a maximum N recovery rate of approximately 154 g $m^{-2}{}_D{}^{-1}$. In contrast, S2 exhibited markedly superior N recovery performance, achieving a maximum N recovery rate of approximately 237 g $m^{-2}{}_D{}^{-1}$.

Based on the graphical representations, mathematical models best fitting the behavior of S1 and S2 were obteined. The mathematical model for S1 is presented in Eq. (6):

$$\text{N recovery rate (g m}^{-2}\text{ d}^{-1}) = 34.76 - 0.82*\text{TAN} + 0.39*\text{time} + 0.37*\text{TAN}^2 - 0.003*\text{TAN}*\text{time} - 0.001*\text{time}^2 \quad (6)$$

The mathematical model for S2 is presented in Eq. (7):

$$\text{N recovery rate (g m}^{-2}\text{ d}^{-1}) = -136.55 + 55.36*\text{TAN} + 1.07*\text{time} - 1.61*\text{TAN}^2 - 0.13*\text{TAN}*\text{time} - 0.0005*\text{time}^2 \quad (7)$$

In both equations TAN stands for initial TAN concentration (g L^{-1}) and time stands for time test (min). The R^2 for S1 was 0.8654 and the mean square error (MSE) was 9.7815. For S2, R^2 was 0.9192 and the MSE was 15.7315.

An optimization analysis was performed by applying partial differentiation techniques to the multivariate regression model. This methodology involved identifying the stationary points of the function by solving the S1 and S2 of equations where the partial derivatives with respect to initial TAN concentration and time were set to zero. Subject to the established operational domain (TAN: 2.8–17.3 g L^{-1}; time: 60–300 min), the analysis revealed that the theoretical maximum for the N recovery rate was located at the upper boundary of the concentration constraint. For S1, the optimal operating point were thus ascertained to be an initial TAN concentration of 17.3 g L^{-1} and an operating time of 152.4 min, which yielded a maximum predicted N recovery rate of 155.65 g m^{-2} d^{-1}. For S2, the optimal operating point were thus ascertained to be an initial TAN concentration of 14.87 g L^{-1} and an operating time of 60 min, which corresponds to a maximum predicted N recovery rate of 281.2 g m^{-2} d^{-1}. The optimal operating point obtained from the model equations was 1.8 times higher in S2 compared to S1.

When comparing the results with previous studies conducted with synthetic manure at concentrations ranging from 3 to 12 g N L^{-1} [10,17], for the low initial TAN concentrations (approx. 3 g L^{-1}, similar to C1), the referenced studies reported N recovery rates of 6–7 g $m^{-2}d^{-1}$ (Soto--Herranz et al., 2021a). In comparison, S1 achieved substantially higher rates, fluctuating between 53.0 and 77.7 g N m^{-2} D^{-1}, while the performance of S2 was even better, yielding rates of up to 119.4 g N m^{-2} D^{-1}. This represents an approximate 10-fold and 17-fold increase in performance for S1 and S2, respectively, compared to previous studies. This demonstrates that the novel GPM system design facilitates a significantly enhanced mass transfer of ammonia.

This trend continued at medium initial TAN concentrations (approx. 6 g L^{-1}, similar to C2), where prior research established a performance range of 13–25 g N $m^{-2}d^{-1}$ [10,17]. Notably, the upper end of this range (24–25 g N m^{-2} d^{-1}) was obtained through the optimization of parameters such as acid flow rate. Nevertheless, both systems in the present study demonstrated markedly superior performance, with S1 yielding rates of 58.6–69.1 g N m^{-2} d^{-1} and S2 achieving rates between 125.0 and 147.3 g N m^{-2} d^{-1}. These results indicate that even with optimized operational parameters, the configurations used in the reference studies did not reach the efficiency levels of the proposed GPM systems.

A similar disparity was observed at high initial TAN concentrations (approx. 12 g L^{-1}), where the literature reported a maximum N recovery rate of 19–34 g N m^{-2} d^{-1}. In this high-concentration regime, the performance of the proposed systems herein was particularly notable; S1 peaked at 154.3 g N m^{-2} d^{-1}, while S2 achieved a remarkable maximum of 237.3 g N m^{-2} d^{-1}. The peak performance of S2 is exceptionally significant, as the achieved rate of 237.3 g m^{-2} d^{-1} is almost identical to the highest recovery rate of 237.0 g m^{-2} d^{-1} reported for a synthetic solution in the referenced study. This finding suggests that the design of S2 is so highly optimized that it can achieve a N recovery flux with real, buffered manure that is comparable to the upper performance limit observed under idealized laboratory conditions. This superior efficiency is attributed to a design that promotes a much more effective mass transfer of ammonia.

Previous studies using GPM to recover N from N-rich atmospheres using a cartridge with the gas cycling around the outside of the membrane reported N recovery rates in the range of 163–237 8 g m^{-2} d^{-1} [18]. These ratios are similar to those obtained in this study but it must be taken into account that a synthetic ammonia solution was used in those previous studies.

When pig manure was used as N-emitting solution using different GPM configurations maximum N recovery rates of 18.8 g m^{-2} d^{-1} [24] and 73.2 g m^{-2} d^{-1} [18] were obtained. The former one used a GPM system with recirculation of the acidic trapping solution and gas circulation while the latter used a GPM system based on a cartridge with gas cycling through the outside of the membrane.

Based on research conducted at pilot plant scale, the study by Soto-Herranz [15] evaluated the long-term performance of pilot plants in swine and poultry farm atmospheres, operating for 232 and 256 days, respectively. The study reported a maximum N recovery rate of 28.6 g m^{-2} d^{-1} for the poultry operation, while the rate for the swine farm was substantially lower at 2.3 g m^{-2} d^{-1}. In a different pilot-scale investigation, Rothrock [25] used flat membranes to treat poultry litter and achieved N recovery rates of 28.62 g m^{-2} d^{-1}. The performance of S2 would represent a significant leap forward in the efficiency of ammonia recovery in N-rich atmospheres. The achieved recovery rates far surpassed the performance benchmarks established in previous studies. This substantial improvement is not merely incremental but is directly attributable to the system's novel design, which is engineered to maximize mass transfer to a degree not previously documented. Therefore, the configuration of S2 establishes a new and much higher standard for what is achievable in GPM technology for ammonia recovery in N-rich atmospheres.

4. Conclusions

Two innovative gas-permeable membrane (GPM) systems, designated System 1 (external gas flow from GPM) and System 2 (internal gas flow from GPM), were designed and evaluated for their effectiveness in recovering nitrogen from ammonia-rich atmospheres. A comparative analysis revealed that while both configurations were functional, their performance efficiencies were significantly different.

The internal gas flow configuration, System 2, demonstrated a markedly superior performance, achieving a peak nitrogen (N) recovery rate of up to 237.3 g m^{-2} d^{-1}. In contrast, the maximum recovery rate achieved by System 1 was 154.3 g m^{-2} d^{-1}. This performance disparity is

particularly noteworthy when considering the operational time: System 2 achieved its substantially higher peak rate in only 60 min, half the time required for System 1 to reach its lower optimum.

Furthermore, mathematical models were developed to characterize the performance of each system. An optimization analysis of these models corroborated the empirical findings, revealing that the theoretical optimal operating point for System 2 was 1.8 times higher than that of System 1. This study conclusively demonstrates the high potential of the internal gas flow GPM configuration for developing highly efficient technologies for nitrogen recovery from ammonia-rich environments, such as those found in livestock operations.

CRediT authorship contribution statement

Paula Calvo-de Diego: Writing – original draft, Visualization, Validation, Software, Methodology, Investigation, Formal analysis, Data curation, Conceptualization. **María Cruz García-González:** Writing – review & editing, Validation, Resources, Project administration, Funding acquisition. **Mercedes Sánchez-Báscones:** Writing – review & editing, Visualization, Validation, Resources, Funding acquisition. **Beatriz Molinuevo-Salces:** Writing – review & editing, Visualization, Validation, Supervision, Software, Resources, Project administration, Methodology, Investigation, Funding acquisition, Data curation, Conceptualization.

Declaration of competing interest

The authors declare the following financial interests/personal relationships which may be considered as potential competing interests: Beatriz Molinuevo Salces reports financial support was provided by University of Valladolid. Beatriz Molinuevo Salces reports financial support was provided by Spanish National Research Council. If there are other authors, they declare that they have no known competing financial interests or personal relationships that could have appeared to influence the work reported in this paper.

Acknowledgements

This work has been supported by the European Union under the Project Life GREEN AMMONIA [LIFE20-ENV/ES/000858]; B. Molinuevo-Salces thanks AEI for funding, through RYC-2020-029030-I/AEI/10.13039/501100011033.

Data availability

Data will be made available on request.

References

[1] European Environment Agency (EEA). Harm to human health from air pollution in Europe: burden of disease, 2022. https://www.eea.europa.eu/publications/harm-to-human-health-from-air-pollution/. (accessed on 10 September 2025).
[2] European Union, Directive (EU) 2016/2284 of the European Parliament and of the Council of 14 December 2016 on the reduction of national emissions of certain atmospheric pollutants, Off. J. Eur. Union (2016). https://eur-lex.europa.eu/eli/dir/2016/2284/oj/eng (accessed on 10 September 2025).
[3] EC, 2022. Report from the Commission to the European Parliament, the Council, the European Economic and Social Committee and the Committee of the Regions 'Third Clean Air Outlook' (COM(2022) 673 final). https://www.eumonitor.eu/9353000/1/j9vvik7m1c3gyxp/vlypiajh6khl. (accessed on 10 September 2025).
[4] European Commission. Zero pollution Action Plan. COM(2021) 400 final, 2021. https://www.eea.europa.eu/en/european-zero-pollution-dashboards/indicators/ammonia-emissions-from-agriculture-and-other-sources-indicator. (accessed on 15 September 2025).
[5] Common Agricultural Policy (CAP) and climate, which evaluates the CAP Strategic Plans for 2023–2027. https://agriculture.ec.europa.eu/common-agricultural-policy/cap-overview/cap-glance_es. (accessed on 17 September 2025).
[6] A. Finzi, A.H. Vazifehkhoran, E. Dinuccio, R. Ambrosini, G. Provolo, Acidification of livestock slurry and digestate to reduce NH3 emissions: predicting needed H2SO4 dosage and pH trends over time based on their chemical-physical composition, Biosyst. Eng. 240 (2024) 1–13, https://doi.org/10.1016/j.biosystemseng.2024.02.012.
[7] D. Georgiou, V. Liliopoulos, A. Aivasidis, Upgrading of biogas by utilizing aqueous ammonia and the alkaline effluent from air-stripping of anaerobically digested animal manure. Application on the design of a semi-industrial plant unit, J. Water Process Eng. 36 (2020) 101318, https://doi.org/10.1016/j.jwpe.2020.101318.
[8] K. Barbusiński, K. Urbaniec, D. Kasperczyk, M. Thomas, Biofilters versus bioscrubbers and biotrickling filters: state-of-the-art biological air treatment. From Biofiltration to Promising Options in Gaseous Fluxes Biotreatment, Elsevier, 2020, pp. 29–51, https://doi.org/10.1016/B978-0-12-819064-7.00002-9.
[9] Ł. Wlazło, B. Nowakowicz-Dębek, J. Kapica, M. Kwiecień, H. Pawlak, Removal of ammonia from poultry manure by aluminosilicates, J. Environ. Manage. 183 (2016) 722–725, https://doi.org/10.1016/j.jenvman.2016.09.028.
[10] M. Soto-Herranz, M. Sánchez-Báscones, J.M. Antolín-Rodríguez, M.B. Vanotti, P. Martín-Ramos, Effect of acid flow rate, membrane surface area, and capture solution on the effectiveness of suspended gpm systems to recover ammonia, Membranes 11 (7) (2021) 538, https://doi.org/10.3390/membranes11070538.
[11] A. Zarebska, D. Romero Nieto, K.V. Christensen, L. Fjerbæk Søtoft, B. Norddahl, Ammonium fertilizers production from manure: a critical review, Crit. Rev. Environ. Sci. Technol. 45 (14) (2015) 1469–1521, https://doi.org/10.1080/10643389.2014.955630.
[12] B. Molinuevo-Salces, B. Riaño, M.B. Vanotti, D. Hernández-González, M.C. García-González, Pilot-scale demonstration of membrane-based nitrogen recovery from swine manure, Membranes 10 (10) (2020) 270, https://doi.org/10.3390/membranes10100270.
[13] P. Cao, C. Lu, Z. Yu, Historical nitrogen fertilizer use in agricultural ecosystems of the contiguous United States during 1850–2015: application rate, timing, and fertilizer types, Earth Syst. Sci. Data 10 (2) (2018) 969–984, https://doi.org/10.5194/essd-10-969-2018.
[14] Fertilizers Europe, energy cost. https://www.fertilizerseurope.com/industry-competitiveness/energy-cost/, 2023 (accessed on 16 September 2025).
[15] M. Soto-Herranz, M. Sánchez-Báscones, J.M. Antolín-Rodríguez, P. Martín-Ramos, Pilot plant for the capture of ammonia from the atmosphere of pig and poultry farms using gas-permeable membrane technology, Membranes 11 (11) (2021) 859, https://doi.org/10.3390/membranes11110859.
[16] M. Soto-Herranz, M. Sánchez-Báscones, J.M. Antolín-Rodríguez, P. Martín-Ramos, Reduction of ammonia emissions from laying hen manure in a closed composting process using gas-permeable membrane technology, Agronomy 11 (12) (2021) 2384, https://doi.org/10.3390/agronomy11122384.
[17] M. Soto-Herranz, M. Sanchez-Bascones, J.M. Antolin-Rodriguez, P. Martin-Ramos, Evaluation of different capture solutions for ammonia recovery in suspended gas permeable membrane systems, Membranes 12 (2022) 572, https://doi.org/10.3390/membranes12060572.
[18] P. Calvo-de Diego, M.C. García-González, M. Sánchez-Báscones, B. Molinuevo-Salces, Developing a new system based on membranes for Ammonia recovery from the atmosphere: effect of operation time and manure temperature, Agronomy 15 (5) (2025) 1109, https://doi.org/10.3390/agronomy15051109.
[19] B. Riaño, B. Molinuevo-Salces, M.B. Vanotti, M.C. García-González, Effect of operational conditions on Ammonia recovery from simulated livestock wastewater using gas-permeable membrane technology, Environments 9 (6) (2022) 70, https://doi.org/10.3390/environments9060070.
[20] O. El bied, M.A.T. Turbí, A. García-Valero, Á.F. Cano, J.A. Acosta, Mitigating ammonia, methane, and carbon dioxide emissions from stored pig slurry using chemical and biological additives, Water 15 (23) (2023) 4185, https://doi.org/10.3390/w15234185.
[21] M.C. García-González, M.B. Vanotti, A.A. Szogi, Recovery of ammonia from swine manure using gas-permeable membranes: effect of aeration, J. Environ. Manage. 152 (2015) 19–26, https://doi.org/10.1016/j.jenvman.2015.01.013.
[22] L. Wu, H. Li, Y. Zhou, Z. Shen, J. Zuo, Independent of alkalinity addition: ammonia recovery via gas permeable membranes driven by self-sustained alkalinity in anaerobic digestate with low-rate aeration, J. Water Process Eng. 74 (2025) 107848, https://doi.org/10.1016/j.jwpe.2025.107848.
[23] S. Calvet, J. Hunt, T.H. Misselbrook, Low frequency aeration of pig slurry affects slurry characteristics and emissions of greenhouse gases and ammonia, Biosyst. Eng. 159 (2017) 121–132, https://doi.org/10.1016/j.biosystemseng.2017.04.011.
[24] M. Soto-Herranz, M. Sánchez-Báscones, M.C. García-González, P. Martín-Ramos, Comparison of the Ammonia trapping performance of different gas-permeable tubular membrane system configurations, Membranes 12 (2022) 1104, https://doi.org/10.3390/membranes12111104.
[25] M.J. Rothrock Jr., A.A. Szögi, M.B. Vanotti, Recovery of ammonia from poultry litter using gas-permeable membranes, Trans. ASABE 53 (2010) 1267–1275, https://doi.org/10.13031/2013.32591.